Migration of Retinal Cells through a Perforated Membrane: Implications for a High-Resolution Prosthesis

Daniel Palanker,[1,2] *Philip Huie,*[1,2] *Alexander Vankov,*[2] *Robert Aramant,*[3] *Magdalene Seiler,*[3,4] *Harvey Fishman,*[1] *Michael Marmor,*[1] *and Mark Blumenkranz*[1]

Purpose. One of the critical difficulties in design of a high-resolution retinal implant is the proximity of stimulating electrodes to the target cells. This is a report of a phenomenon of retinal cellular migration into a perforated membrane that may help to address this problem.

Methods. Mylar membranes with an array of perforations (3–40 μm in diameter) were used as a substrate for in vitro retinal culture (chicken, rats) and were also transplanted into the subretinal space of adult RCS rats. A membrane was also constructed with a seal on one side to restrict the migration.

Results. Retinal tissue in vitro grew within 3 days through perforations of greater than 5 μm in diameter when the membranes were positioned on the photoreceptor side, but no migration occurred if the implant was placed on the inner retinal surface. Histology with light microscopy and transmission electron microscopy (TEM) demonstrated that migrating cells retain neuronal structures for signal transduction. Similar growth of RCS rat retinal cells occurred in vivo within 5 days of implantation. A basal seal kept the migrating tissue within a small membrane compartment.

Conclusions. Retinal neurons migrate within a few days into perforations (>5 μm in diameter) of a membrane placed into the subretinal space. This may provide a means of gaining close proximity between electrodes in a retinal prosthetic chip and target cells, and thus allow a greater density of stimulating elements to subserve higher resolution. Further studies are needed to explore the long-term stability of the retinal migration. (*Invest Ophthalmol Vis Sci.* 2004;45:3266–3270) DOI:10.1167/iovs.03-1327

As the population ages, vision loss from retinal diseases is becoming a major public health issue. Two degenerative retinal disorders are the current focus of retinal prosthetic work: retinitis pigmentosa (RP) and age-related macular degeneration (AMD). In these diseases, the photoreceptor layer of the retina degenerates, yet the "processing circuitry" and "wiring" are at least to some degree preserved. If one could bypass the photoreceptors and directly stimulate the inner retina with visual signals, one might be able to restore sight.[1–4] Some first steps have been taken toward the development of an electronic retinal prosthesis. Human patients stimulated with an array of 16 to 20 electrodes of 0.4 mm in size can recognize reproducible visual percepts,[3,5] which gives hope that with some learning and image processing, the patients might be able to get used to this type of stimulation.[6] Electrical stimulation of neural cells in the retina has been achieved with an array of electrodes positioned on either the inner[4,5,7,8] or outer side of retina (Sachs HG, et al. *IOVS* 2000;41:ARVO Abstract 533).[9,10] Setting the electrodes into the subretinal space with electrical stimulation of the inner retinal cells, although surgically challenging, has the potential advantage that earlier signal processing in the retina may be partially preserved, relative to the excitation of ganglion cells with electrodes positioned on the epiretinal side. These pioneering implants are a long way from the number and density of stimulating pixels needed to achieve functional levels of vision. (We must emphasize though that high density of retinal stimulation is only one of the requirements for restoring useful visual perception.)

Implantation is worth the risk for patients with low visual acuity (e.g., 20/400) only if it provides substantial improvement. A visual acuity of 20/80 corresponds geometrically to a pixel size of 20 μm and pixel density of 2500 pixels/mm^2.[11] To achieve such high-resolution stimulation, it is necessary to bring the prosthetic electrodes close to the target cells. This problem has hardly been addressed. Simple placement of a flat electrode array on, or under, the retina always leaves a large distance between electrodes and cells, because the inner limiting membrane and nerve fiber layer intervene in the case of epiretinal approach, and photoreceptor remnants interfere in the case of subretinal implantation. In addition, diseased retina may have uneven thickness or a wavy structure. Large distances between the cells and electrodes require a high charge density and power for cell stimulation[11] and result in cross-talk between closely spaced electrodes. High charge density and power can lead to erosion of electrodes and excessive heating of the tissue, all of which limit spatial resolution. Furthermore, any variability in the distance between electrodes and cells in different parts of the implant will result in variations of the stimulation threshold, making it necessary to adjust the signal intensity in each pixel. We have recently calculated[11] that for chronic stimulation with a pixel density of 400 pixels/mm^2, which geometrically corresponds to visual acuity of 20/200, the electrodes need to be within 15 to 20 μm of the target neurons. For visual acuity of 20/80, the separation between electrodes and target cells should not exceed 7 μm. Thus, ensuring a very close proximity of retinal cells to the stimulating electrodes is one of the important issues, and challenges, in the design of a high-resolution retinal prosthesis.

From the [1]Department of Ophthalmology, School of Medicine, and the [2]W. W. Hansen Experimental Physics Laboratory, Stanford University, Stanford, California; and the Doheny Retina Institute, Departments of [3]Ophthalmology and [4]Cell and Neurobiology, School of Medicine, University of Southern California, Los Angeles, California.

Supported in part by the Stanford University Bio-X grant and by VISX Inc. The work at Doheny was supported by an anonymous sponsor, the Foundation for Fighting Blindness, and National Eye Institute Core Grant EY03040.

Submitted for publication December 9, 2003; revised March 31, 2004; accepted April 27, 2004.

Disclosure: **D. Palanker**, VISX Inc. (F, P); **P. Huie**, VISX Inc. (F, P); **A. Vankov**, VISX Inc. (F, P); **R. Aramant**, None; **M. Seiler**, None; **H. Fishman**, VISX Inc. (F, P); **M. Marmor**, None; **M. Blumenkranz**, VISX Inc. (F, P)

The publication costs of this article were defrayed in part by page charge payment. This article must therefore be marked "*advertisement*" in accordance with 18 U.S.C. §1734 solely to indicate this fact.

Corresponding author: Daniel Palanker, W. W. Hansen Experimental Physics Laboratory, Stanford University, Stanford, CA 94305-4085; palanker@stanford.edu.

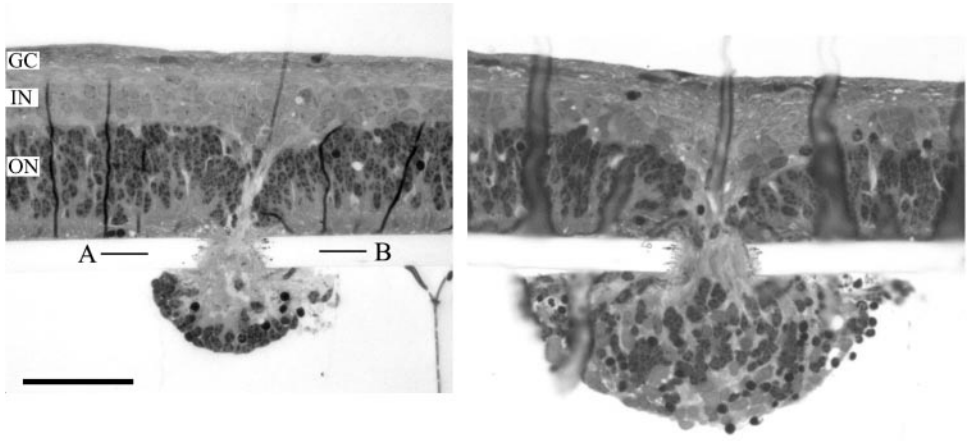

FIGURE 1. Light micrographs of the histologic sections of the P7 rat retina 72 hours after explantation onto 13-μm-thick perforated mylar membrane. Apertures were (*left*) 16 and (*right*) 26 μm in diameter. The cellular migration was greater through the larger aperture. *Left*, A, B: line of sectioning for TEM imaging of the tuft shown in Figure 2. Retinal layers in all figures are labeled with the two-letter code as follows: GC, ganglion cell; IP, inner plexiform; IN, inner nuclear; OP, outer plexiform; ON, outer nuclear; PE, pigmented epithelium; CH, choroid; M, migrated tissue. Scale bar, 50 μm.

Our laboratory is exploring several approaches to ensure proximity of neural cells to stimulating electrodes (Huie P, et al. *IOVS* 2002;43:ARVO E-Abstract 4475; Huie P, et al. *IOVS* 2003;44:ARVO E-Abstract 5055).[12] In this article we report that a subretinal placement of a perforated membrane prompted a migration of retinal cells through the perforations.

MATERIALS AND METHODS

In Vitro Experiments

Mylar membrane, 13 μm in thickness, was perforated on an inverted microscope using the tightly focused beam of a picosecond Ti-Sapphire laser (Spitfire; Spectra Physics, Inc., Santa Clara, CA). Aperture sizes varied in the range of 3 to 40 μm. The surface of the membrane was treated with 0.1 mg/mL poly-L-lysine (P2636; Sigma-Aldrich, St. Louis, MO) and 0.4 mg/mL laminin diluted in neurobasal medium (L2020; Sigma-Aldrich and Invitrogen-Gibco, Carlsbad, CA, respectively). The perforated membranes were affixed atop polystyrene rings mounted at the center of Petri dishes to form an inner chamber and a surrounding outer chamber. The inner and outer chambers were filled with the same culture medium. Some membranes were constructed with an additional mylar basal membrane, with and without 3-μm perforations to limit retinal cellular migration.

Animals were used in accordance with the ARVO Statement for the Use of Animals in Ophthalmic and Vision Research. Retinas were harvested from postnatal day (P)7 Sprague-Dawley rat pups (20 samples) and from embryonic day (E)16 to E18 chicken embryos (6 samples). After removal of the inner limiting membrane (ILM) by peeling, the retinas were positioned onto perforated mylar membranes and incubated for 72 hours in growth medium that consisted of neurobasal medium, pen/strep, insulin, L-glutamine, Sato supplement, and B27. Each membrane had an array of 20 to 50 apertures (4 $\times$ 5 to 5 $\times$ 10). Tuft growth through the perforations was visually monitored with an inverted microscope (TS100; Nikon, Tokyo, Japan) and then processed for histologic examination.

In Vivo Experiments

Five albino RCS rats, derived from the breeding colony at Doheny Eye Institute received implants in one eye at the age of 63 days. The implantation procedure have been described in detail elsewhere.[13] In anesthetized rats (ketamine 37.5 mg/kg; xylazine 5 mg/kg), a small incision ($\sim$1 mm) was cut transsclerally behind the pars plana of the host eye, and the perforated mylar film (0.8 $\times$ 1.5 mm in size) was placed into the subretinal space, in the back of the eye near the optic disc in the nasal or superior nasal quadrant of the host, using a custom-made implantation tool. Each implant had an array of 28 apertures (4 $\times$ 7). Placement of the transplants was evaluated after each surgery by fundus examination. One surgery failed, and the other four rats were killed for histologic analysis in the following order: Two rats were killed on the fifth day, one on the seventh day, and one on the ninth day after surgery.

Histology

Retina/perforated membranes in the in vitro experiments and the enucleated eyes in the in vivo experiments were immersion fixed in 2.5% glutaraldehyde/2.0% paraformaldehyde in 0.1 M sodium cacodylate buffer (pH 7.4) or in 0.1 M sodium phosphate buffer (pH 7.2). The cornea in the RCS rat eyes was removed 20 to 50 minutes later, and the eyes were postfixed overnight at 4°C. The tissue was washed in 0.1 M sodium cacodylate or 0.1 M sodium phosphate, osmicated in 2% osmium tetroxide, dehydrated in a series of ethanols and washed in anhydrous propylene oxide.

The tissues were embedded (either EMbed 812; Electron Microscopy Sciences, Port Washington, PA, or LX-112; Ladd Research Industries, Inc., Burlington, VT). One-micrometer sections for light microscopy or 100-nm sections for transmission electron microscopy were cut on an ultramicrotome (Reichert-Jung Ultracut E; Leica, Deerfield, IL). Sections for light microscopy were stained with toluidine blue and photographed on a microscope (Eclipse E1000; Nikon). Thin sections for electron microscopy were stained with uranyl acetate and lead citrate. Transmission electron micrographs were then collected (model 1230; JEOL USA., Inc., Peabody, MA).

RESULTS

In vitro experiments with 14 P7 rats were performed with 12 membranes (each having an array of 28–40 apertures of 3–30 μm in size, total 383 apertures) placed subretinally—photoreceptor-side down—and two membranes (having arrays of 28 and 30 apertures of 5–30 μm in size) epiretinally. Seventy-two hours after explantation, migration was observed in 88% of the subretinal apertures larger than 5 μm in size. Migration did not occur through the apertures of 5 μm or smaller, nor did it occur with any aperture sizes after epiretinal placement. In vitro experiments with chicken retina have been performed with six membranes each having 40 apertures of 10 to 20 μm in size, all of which where placed subretinally. At 72 hours after the explantation migration was observed in 81% of the apertures.

Histologic results obtained in vitro with the P7 rat retinas are shown in Figures 1, 2 and 3. Migration of cells from the outer nuclear layer, outer plexiform layer, and inner nuclear layer progressively increased with aperture sizes above 5 μm. The cellular invasion of the aperture appeared to include both glial and neural cellular elements. As shown in Figure 1, (right), the extent of tissue migration increased with the size of the

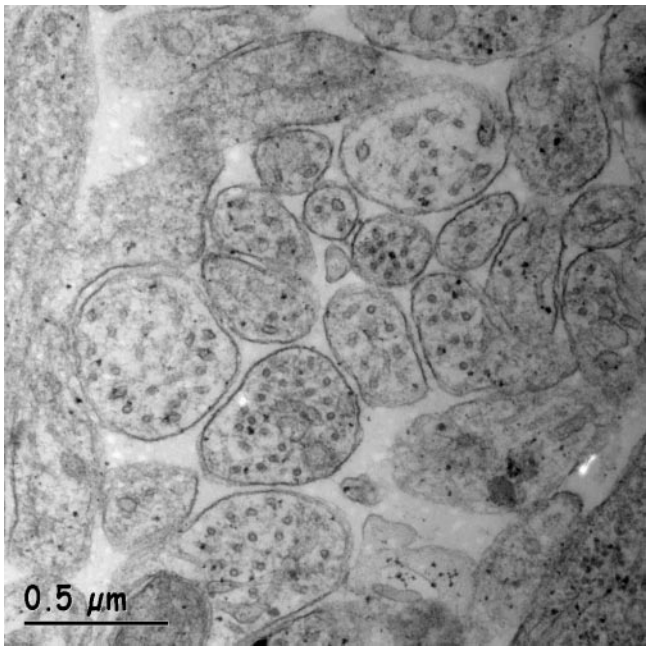

FIGURE 2. Transmission electron microscopy. Cross-section of nerve axons or dendrites within a channel connecting cells within the retina to a migrating tuft. Scale bar, 0.5 μm.

aperture. A transmission electron micrograph of a section through an aperture (similar to the line A-B, in Fig. 1, left) is shown in Figure 2 and demonstrates the presence of neuronal processes (axons or dendrites) connecting the migrating cells. These findings indicate the possibility of signal transmission between stimulated cells in the aperture and cells in the rest of the retina.

Figure 3 demonstrates a typical example of culturing the rat retina upside down—nerve fiber layer toward the membrane—that did not result in cellular migration, even though the ILM was peeled off.

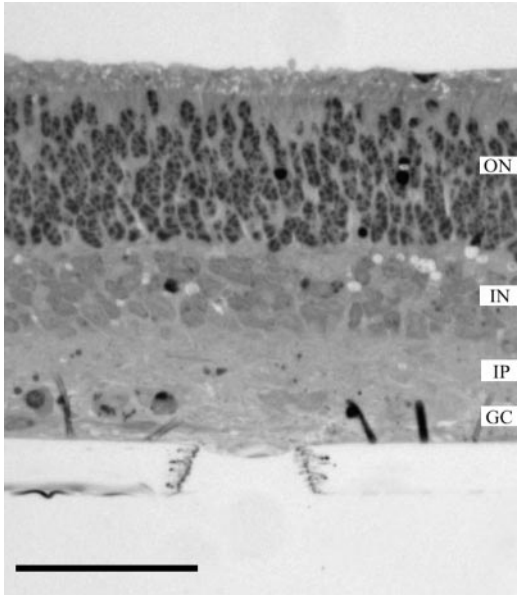

FIGURE 3. P7 rat retina cultured for 72 hours in vitro upside down—that is, with the nerve fiber layer adjacent to the perforated membrane. No cellular migration was observed through pore sizes up to 23 μm. For abbreviations, see Figure 1. Scale bar, 50 μm.

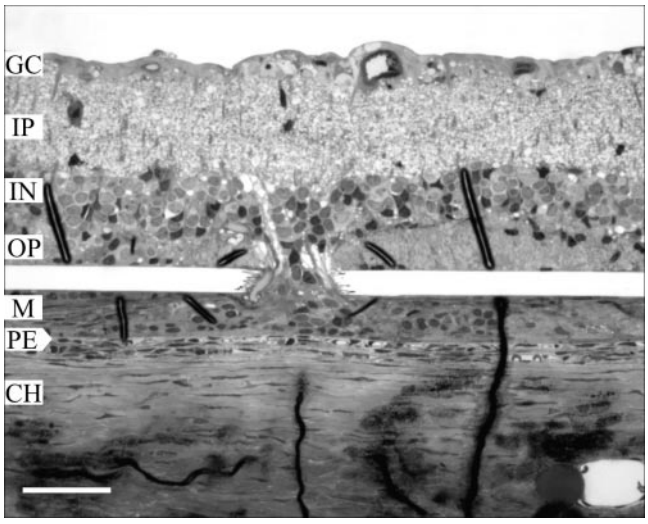

FIGURE 4. Histologic section of the RCS rat retina 9 days after implantation of the perforated mylar membrane into the subretinal space. Retinal tissue migrated through the hole and spread between the RPE and the membrane. For abbreviations, see Figure 1. Scale bar, 50 μm.

The RCS rat was chosen as a model for in vivo experiments, since the retina is vascularized and the photoreceptors degenerate as in RP. Results of the experiments with subretinal mylar films perforated with 4 × 7 arrays of apertures of 15 to 40 μm were analyzed histologically in four eyes from the animals killed 5, 7, and 9 days after the implantation. A robust migration of the inner nuclear layer was observed in all 36 apertures analyzed histologically (Figs. 4 and 5). In several apertures, we also observed a migration of retinal capillaries into the pore (Fig. 5).

Because unlimited tissue migration through a membrane could be problematic (draining retinal cells and proliferating under the prosthesis), we explored the placement of perforated membranes with a basal seal to prevent growth out of the bottom of the membrane (Fig. 6). To test whether diffusion of nutrients is essential for migration some of the basal mylar membranes where perforated, and some were not. The experiments were performed in vitro with six cultured P7 rat retinas, with six devices, each having an array of 15 (5 × 3) chambers.

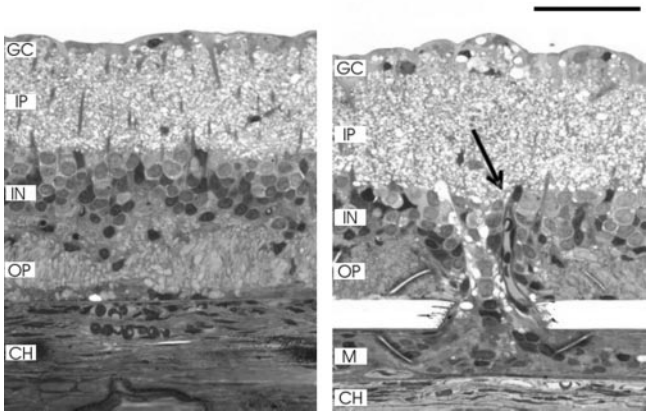

FIGURE 5. Histologic sections of the RCS rat retina 9 days after implantation. *Left:* normal appearance of the RCS rat retina far from the implant; *right:* retinal tissue migrated through the aperture of 40 μm and spread between the RPE and the membrane. *Arrow*: blood capillary migrating into the pore. For abbreviations, see Figure 1. Scale bar, 50 μm.

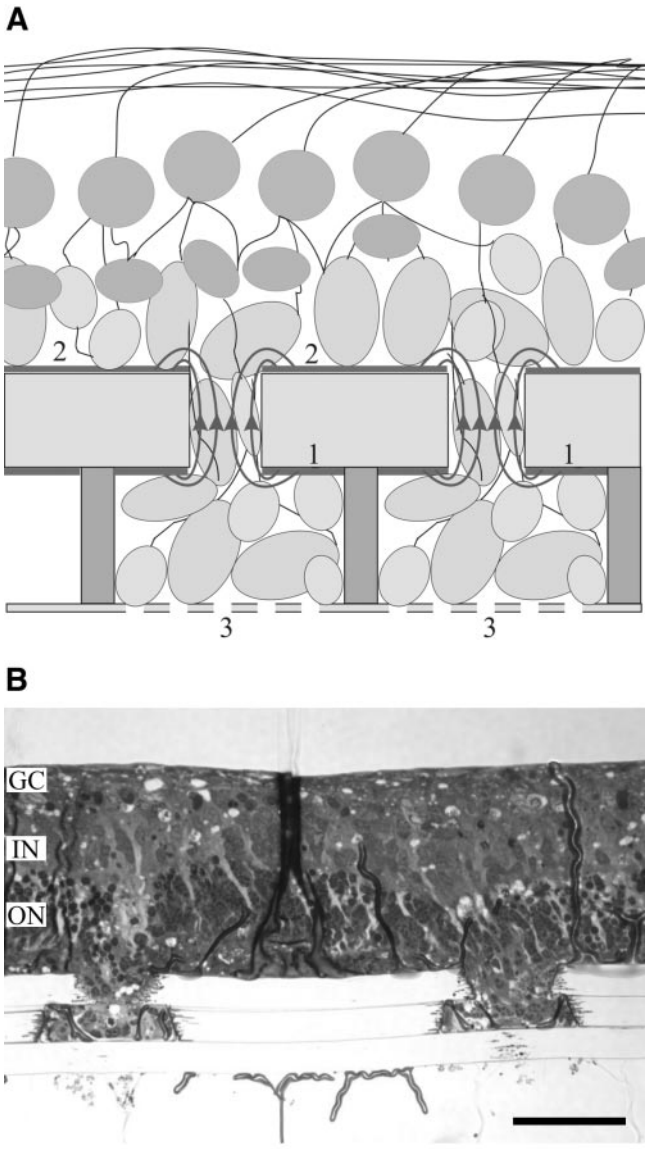

FIGURE 6. **(A)** Schematic representation of a three-layered membrane with an entry channel on top, a wider inside chamber, and a fenestrated membrane (3) at the bottom to limit cellular migration. Stimulating voltage was applied between an inner electrode (1) and a common return electrode (2). **(B)** Rat retina grown on the three-layered structure for 7 days in vitro. Retinal cells migrated through the 20- and 35-μm holes into the middle chambers 60 μm in width, but could not penetrate the 3-μm holes in the lower membrane. For abbreviations, see Figure 1. Scale bar, 50 μm.

Nine of 15 chambers in each device had small perforations (3 μm) at the basal membrane, and six did not. When retinas were cultured over these three-layer structures for 7 to 14 days, tissue was observed to migrate into 94% of chambers with basal perforations (Fig. 6B), and 87% of those with no basal perforations (Fig. 7). One can see in both Figures 6 and 7 that the nuclei of the outer nuclear layer migrated into the chamber.

DISCUSSION

The remodeling and potential plasticity of adult retina after injury or degeneration of the photoreceptors has been documented now by many investigators.[14–19] There is not only neuronal proliferation but also a growth of non-neural cells, including Müller cells and blood vessels.[14–19] After retinal reattachment, Müller cell processes and displaced photoreceptor nuclei can move into the subretinal space and spread laterally.[15,16] The cell processes of displaced Müller cells can form scaffolds that aid in the migration of other retinal neural cells,[17] and these may be facilitating the neural retinal migration in our case. Another mechanism of retinal migration involves permeation of the RPE cell extensions deep into the neural retina, and the attraction of small blood vessels from the ganglion cell layer.[18] However, RPE cannot be responsible for the retinal migration we observed in vitro, since no RPE was present in that case. The participation of the RPE cells in vivo will also be prevented if a membrane seals the bottom of an implant, as shown in Figures 6 and 7.

The relevance of these observations to prosthetic chip technology is that, whereas close spacing of electrodes on a chip is needed for high resolution, there is electrode cross-talk or excessive power requirements, unless the target neurons come within a few micrometers of the stimulus area. Because retinal neurons enter a perforated membrane, as we have shown, they would enter a chip that has stimulating electrodes in perforations (as suggested in Fig. 6A). This would bring the electrodes and neurons into close proximity, which is necessary for high-resolution performance. Penetration of cells into the pores of an implant may also help to achieve a firm mechanical anchoring of the device to tissue.

Effect of cellular migration can also be used with an implant having an array of thin protruding electrodes insulated at their sides and exposed at the tops. When positioned under the retina, the cells migrate into the empty spaces between the electrodes, thus assuring penetration of the electrodes into the retina without high pressure and associated risk of mechanical injury. The depth of penetration is determined by the length of the electrodes. The approaches based on pores and on protruding electrodes are complimentary: In the first case the actively migrating cells penetrate into the pores and are stimulated. In the second case the actively migrating cells move toward the bottom of an implant, while the electrodes penetrate deep into the retina approaching the target cells that did not migrate and remained in place.

Major concerns with retinal migration are whether the neural cells that move into the pores will survive for an extended period and whether the organization of the migrated tissue will

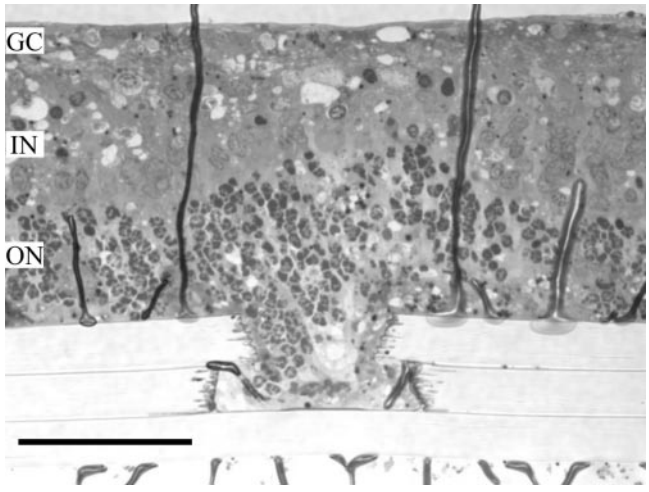

FIGURE 7. Rat retina grown on the three-layered structure for 7 days in vitro. Retinal cells migrated through the 35-μm holes into the middle chambers 60 μm in width, which did not have holes in the lower membrane. For abbreviations, see Figure 1. Scale bar, 50 μm.

change through glial overgrowth or cell death. Studies with nonporous subretinal implants suggest that the Müller cells can migrate and proliferate, making fibrous tissue and changing neuronal configurations.[19,20] Proliferation of the glial cells has also been observed with porous membranes implanted on the epiretinal side (Laube T, et al. IOVS 2000;41:ARVO Abstract 530). We plan to study the long-term behavior of retinal cells migrating into perforated implants and to optimize their structure for preserving neural connections and assuring efficacy of an electric interface. Our purpose in this initial report is simply to alert readers to this intriguing phenomenon of neural ingrowth and to emphasize its potential relevance to prosthetic chip development.

Acknowledgments

Authors thank Kalayaan V. Bilbao and Dimitri Yellachich for help with the rabbit surgery; Zhenhai Chen for help with the rat surgeries; Thomas Guillaume, Yevgeny Freyvert, and Gary Chern for help with membrane fabrication; and Roopa Dalal for histologic preparations.

References

1. Zrenner E. Will retinal implants restore vision? *Science*. 2002;295: 1022–1025.
2. Humayun MS, de Juan E. Artificial vision. *Eye*. 1998;12:605–607.
3. Humayun MS. *Clinical Trial Results with a 16-Electrode Epiretinal Implant in End-Stage RP Patients.* Presented at the First DOE International Symposium on Artificial Sight. Fort Lauderdale, FL: US Department of Energy; 2003:10.
4. Margalit E, Maia M, Weiland JD, et al. Retinal prosthesis for the blind. *Surv Ophthalmol.* 2002;47:335–356.
5. Rizzo JF III, Wyatt J, Loewenstein J, Kelly S, Shire D. Perceptual efficacy of electrical stimulation of human retina with a microelectrode array during short-term surgical trials. *Invest Ophthalmol Vis Sci.* 2003;44:5362–5369.
6. Humayun MS, Weiland JD, Fujii GY, et al. Visual perception in a blind subject with a chronic microelectronic retinal prosthesis. *Vision Res.*, 2003;43:2573–2581.
7. Margalit E, Weiland JD, Clatterbuck RE, et al. Visual and electrical evoked response recorded from subdural electrodes implanted above the visual cortex in normal dogs under two methods of anesthesia. *J Neurosci Methods*. 2003;123:129–137.
8. Humayun MS, de Juan E, Weiland JD, et al. Pattern electrical stimulation of the human retina. *Vision Res.* 1999;39:2569–2576.
9. Zrenner E, Gekeler F, Gabel VP, et al. Subretinal microphotodiode arrays to replace degenerated photoreceptors? *Ophthalmologe.* 2001;98:357–363.
10. Stett A, Barth W, Weiss S, Haemmerle H, Zrenner E. Electrical multisite stimulation of the isolated chicken retina. *Vision Res.* 2000;40:1785–1795.
11. Palanker D, Vankov A, Mirkin MV, Fishman HA, Blumenkranz MS, Marmor MF. Physical constraints on the design of a high-resolution electronic retinal prosthesis. *IEEE Trans. Biomed. Eng.* In press.
12. Peterman MC, Mehenti NZ, Bilbao KV, et al. The artificial synapse chip: a flexible retinal interface based on directed retinal cell growth and neurotransmitter stimulation. *Artificial Organs.* 2003; 27:975–985.
13. Aramant RB, Seiler MJ. Retinal transplantation: advantages of intact fetal sheets. *Prog Retin Eye Res*. 2002;21:57–73.
14. Fisher SK, Erickson PA, Lewis GP, Anderson DH. Intraretinal proliferation induced by retinal detachment. *Invest Ophthalmol Vis Sci.* 1991:32:1739–1748.
15. Erickson PA, Fisher SK, Anderson DH, Stern WH, Borgula GA. Retinal detachment in the cat: the outer nuclear and outer plexiform layers. *Invest Ophthalmol Vis Sci.* 1983;24:927–942.
16. Anderson DH, Guerin CJ, Erickson PA, Stern WH, Fisher SK. Morphological recovery in the reattached retina. *Invest Ophthalmol Vis Sci.* 1986. 27:168–183.
17. Sullivan R, Penfold P, Pow DV. Neuronal migration and glial remodeling in degenerating retinas of aged rats and in nonneovascular AMD. *Invest Ophthalmol Vis Sci.* 2003;44:856–865.
18. Villegas-Perez MP, Lawrence JM, Vidal-Sanz M, Lavail MM, Lund RD. Ganglion cell loss in RCS rat retina: a result of compression of axons by contracting intraretinal vessels linked to the pigment epithelium. *J Comp Neurol.* 1998:392:58–77.
19. Marc RE, Jones BW, Watt CB, Strettoi E. Neural remodeling in retinal degeneration. *Prog Retin Eye Res.* 2003;22:607–655.
20. Pardue MT, Stubbs EB, Jr, Perlman JI, Narfstrom K, Chow AY, Peachey NS. Immunohistochemical studies of the retina following long-term implantation with subretinal microphotodiode arrays. *Exp Eye Res.* 2001;73:333–343.